Proceedings of the 28th IEEE
EMBS Annual International Conference
New York City, USA, Aug 30-Sept 3, 2006

A Method for Online Estimation of Human Arm Dynamics

Farid Mobasser and Keyvan Hashtrudi-Zaad
Department of Electrical and Computer Engineering, Queen's University, Kingston, ON, Canada
Email: khz@post.queensu.ca

Abstract— **Human arm dynamics can be used for human body performance analysis or for control of human-machine interfaces. In this paper, a novel method for online estimation of human forearm dynamics using a second-order quasi-linear model is presented. The proposed method uses Moving Window Least Squares to locally identify dynamic parameters for a limited number of operating points in a variable space defined by elbow joint angle and velocity, and the electromyogram signals collected from upper-arm muscles. The dynamic parameters for these limited points are then employed to train a Radial Basis Function Artificial Neural Network to interpolate/extrapolate for online estimates of arm dynamic parameters for other operating points in the variable space. The proposed estimation method is evaluated on a single degree-of-freedom robotic arm.**

I. Introduction

It is known that the impedance of elbow is a function of joint kinematic data such as joint angle and velocity as well as Muscle Activation Levels (MALs) [1], [2], [3], [4]. Considering this fact, a variety of biomechanical models have been developed to predict joint torque from individual muscle forces. Explicit model-based approaches that use muscle Hill model are one group of them [4]. In an alternative approach, elbow joint dynamics have frequently been modelled using second-order quasi-linear dynamics [3], [5]. However, so far most of the effort has only focused on off-line estimation of joint dynamics. Real-time estimation of joint stiffness and damping has been implemented under random perturbations [6] or biased inputs [7]. These operation conditions are not suitable for applications in which applying perturbations in real-time is not feasible, *e.g.* haptics or telerobotics.

This work focuses on online estimation of a time-varying dynamic model of human arm for contact applications where the motion of the arm is limited to elbow movement in the horizontal plane. Towards this end, a second-order quasi-linear model for each operating point in a six dimensional (6D) operational space defined by elbow joint angle and velocity, and electromyogram (EMG) signals from upper-arm muscles is considered. The model parameters are identified for a limited number of points using a Moving Window Least Squares (MWLS) estimation method. The limited number of points is justified as in contact applications the arm workspace and movement is relatively small and slow. A Radial Basis Function Artificial Neural Network (RBFANN) is then trained with the limited points and is utilized for online interpolation/extrapolation of the quasi-linear dynamic model parameters for other operating points, provided upper-arm EMG signals and elbow joint angle and angular velocity.

II. Elbow Joint Dynamics Modelling

Elbow joint dynamics have frequently been modelled using a second-order quasi-linear dynamics [3], [5]

$$T(t) = T^*(t) + [M\ddot{\theta}(t) + B(\boldsymbol{\lambda}(t))\dot{\theta}(t) + K(\boldsymbol{\lambda}(t))\Delta\theta(t)] \quad (1)$$

where $T(t)$ represents the net torque acting about the joint, $T^*(t)$ denotes a background low-frequency torque generated in elbow by direct commend from brain, $\Delta\theta(t)$ is the elbow position displacement about its equilibrium point, M, B and K are inertial, damping and stiffness parameters, and $\boldsymbol{\lambda}(t)$ denotes the "operating point (state)" of the elbow at time t. Since the inertia of the forearm and hand is constant in the entire operating range of elbow, its value is independent of the operating point. It is well known that the impedance of elbow in static posture is a strong function of elbow angle as well as MALs [1], [3], [4]. During motion the impedance is also a function of angular velocity [2]. Therefore, $\boldsymbol{\lambda}(t)$ is determined by upper-arm MALs represented by EMG signals, and elbow angular position and velocity. In our case, considering four EMG signals collected, the variable space is 6D, that is $\boldsymbol{\lambda}(t) = [EMG_i, \theta, \dot{\theta}],\ i = 1, ..., 4$.

III. Impedance Identification Methodology

As mentioned before, for elbow motion in the horizontal plane, joint dynamics is a strong function of the "arm variable" vector $\boldsymbol{\lambda}$(t), *i.e.* MAL of upper-arm muscles (four signals in our case) and joint angle and velocity [1], [3], [4]. Since the forearm physical properties and hand posture do not change in the entire experiment, the moment of inertia of the forearm is constant and is identified independently. We would like to develop an impedance identification methodology that provides an online estimate of operator's arm locally linearized impedance parameters, *i.e.* $B(\boldsymbol{\lambda}(t))$ and $K(\boldsymbol{\lambda}(t))$. Therefore, we divide the 6D "variable space" into a 6D grid spanned by the arm variables. The impedance associated with a limited number of cells are calculated by feeding the measured hand position and force at that operating point to a MWLS least squares algorithm, as shown in Figure 1.

Since the measurement of the impedance parameters for all grid cells is very time consuming and difficult if not impossible, an efficient interpolation/extrapolation method has to be used to predict the impedance parameters in the arm variable space based on the limited number of identified points. In this work, an RBFANN is employed to interpolate/extrapolate the arm impedance in its entire 6D variable space. The network is trained with the limited number of points obtained from least squares. RBFANN has the advantage of minimum

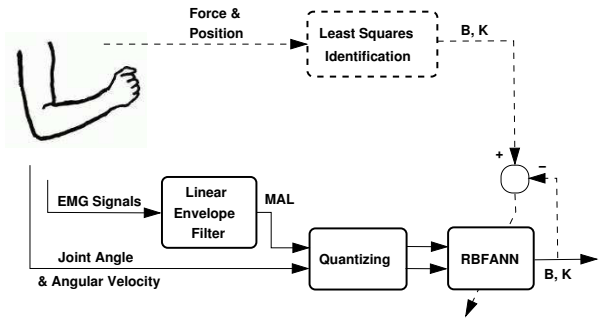

Fig. 1. Block diagram of the proposed method for approximating arm impedance for all operating points using RBFANN. Training process is shown with dashed line.

memory usage for function approximation and has been used significantly for interpolation [8].

In the learning process as shown by dashed lines in Figure 1, the network is trained such that its impedance estimation output for the training points matches the impedance parameters derived from least squares using measured hand position and force. In the operational phase, the EMG signals, the elbow joint angle and angular velocity are quantized and fed to the trained RBFANN to obtain an online estimate of the impedance parameters for current operating points, as shown by solid lines in Figure 1. The details of the described experimental procedure will be explained next.

IV. Experimental Setup and Procedure

Impedance identification experiments were conducted on a single degree-of-freedom (1-DOF) robotic testbed (QArm1) [9], as illustrated in Figure 2. The robotic arm rotates in the horizontal plane and can apply up to 15N/45N continuous/intermittent force to subject's arm. The apparatus is equipped with an ATI Gamma 6-DOF force/torque sensor and an encoder to measure hand force and motor angle. In our experiments, subject's shoulder and wrist were placed in the arm troughs ensuring that the upper-arm was stabilized and the elbow joint axis coincided with the bar rotation axis. Since shoulder joint angle affects the doubly muscles length and thus the impedance of elbow joint, the subject's shoulder was stabilized at 90° abduction, 15° horizontal adduction and neutral pronation-supination. Subjects were asked to relax all muscles not directly involved in elbow flexion/extension. EMG signals were collected from the four muscles biceps brachii, tricpes brachii, brachialis and brachioradialis. Due to the size of biceps and triceps muscles, multiple electrodes were placed at different locations for more accurate MAL estimation. The method proposed in [9] was used for the normalization of EMG measurements. All position, force and EMG data were sampled at *1kHz*.

Experiments were conducted under three condition types as outlined below. In each experiment, the EMG data from the four muscles, the elbow angle, and the subject's force at wrist point were recorded. The experiments were conducted on the right arm of four male subjects with the average age

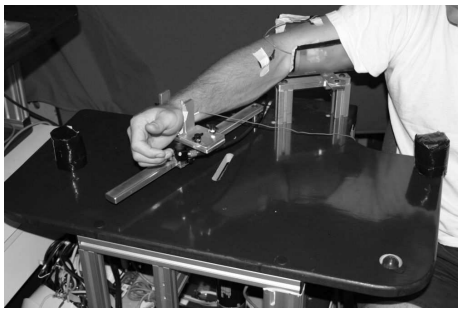

Fig. 2. The 1-DOF experimental setup (QARM1).

of 24. The subjects had no known neuromuscular deficits of the right shoulder, arm or hand. Due to limited space, only a sample of QArm1 applied torque, elbow joint and torque, and EMG signals recorded from subject M1 under experimental condition II are shown in Figure 3.

Experiment type I (Relaxed Muscles): In this condition that lasted for 60 seconds, subjects were asked to relax all upper-arm muscles and do not react to random torque perturbations applied by QArm1.

Experiment type II (Voluntary Constant EMG Posture Control): In this condition, the processed EMG (PEMG) of biceps was shown to subjects on a computer display and they were asked to keep the signal at a displayed constant level [3]. Meanwhile random torque perturbations were applied to subjects' elbow by QArm1 and the subjects were asked to keep their arm angle constant, while concentrating more on PEMG level. This experiment was designed to enforce subjects to control the elbow joint damping and stiffness by co-activating the antagonist muscle pairs. Data was recorded for five elbow angles (45, 20, 0, -20 and -40 flexion) and four PEMG levels (20%, 60%, 90% and 120% of the normalized biceps PEMG level). In general, higher PEMG levels were more challenging to maintain than lower levels.

Experiment type III (Constant Load Posture Control): In this condition, which was also employed in [3], torque perturbations biased with constant load were applied by QArm1 while subjects were asked to keep their arm angle constant. This experiment was designed to identify the elbow joint impedance in the presence of a constant background force applied to the arm. Data was recorded for five elbow angles (40, 20, 0, -20 and -40 flexion) using four constant loads (4.44, 2.22, -2.22 and -4.44 *Nm*.)

The proposed experiments were designed for impedance identification in elbow posture control situation since the operation is slow in contact applications. The identification of elbow impedance in motion control is more challenging due to the motion artifacts induced in EMG measurements, which are caused by the movement of muscles under the electrodes placed on skin.

A. Signal Processing Methods

A 9-tap length median filter was used to remove the spiky noise in measured hand force. The signal bias is removed from the recorded EMG signal, then rectified and passed through a moving average filter with window size of 300 samples [10]. To find the position displacement from the

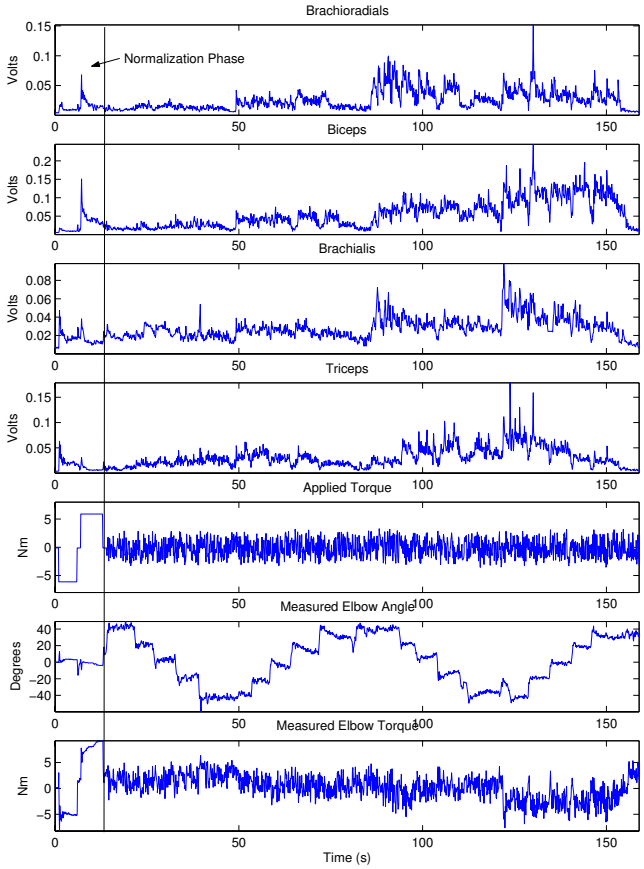

Fig. 3. Sample collected data from subject M1 under experimental condition type II (Voluntary Constant EMG Posture Control).

equilibrium point, that is $\Delta\theta$ in (1), the elbow equilibrium position was calculated using a 2000-tap FIR low-pass filter with cutoff frequency 0.01 *Hz* and shifting back by 1000 samples to cancel the delay caused by filtering. Then the calculated bias is subtracted from the measured angle to compute the position displacements $\Delta\theta$ [6]. The angular velocity and acceleration were derived from pulley angular position and velocity using backward difference differentiation. The angle and the computed velocity and acceleration are passed through a 100-tap moving average filter to remove the effect of quantization noise. To compensate for the delay caused by filtering, the resulted signals were shifted back by half the window size which was 50 samples.

V. Impedance Identification Procedure and Results

In this section, the details of the impedance identification algorithms and experimental results are presented. The identification process is conducted in three phases: i) finding lower arm and hand inertia, ii) using MWLS to identify the arm "stiffness" and "damping" for limited points in the 6D variable space, and iii) using an RBFANN to online estimate the elbow impedance after training the network offline with the above MWLS estimation results.

TABLE I

THE COMPUTED INERTIA FOR FOUR SUBJECTS.

M1	M2	M3	M4
0.0779 kgm^2	0.1030 kgm^2	0.0815 kgm^2	0.1181 kgm^2

A. Lower Arm and Hand Moment of Inertia Identification

Since the forearm physical properties and subject's hand posture do not change in all experiments, the lower arm and hand moment of inertia is almost constant and can be identified independently. To find inertia, subjects were asked to relax all upper-arm muscles in experiment type I, that is $T_h^\star(t) = 0$. Under this condition, inertial effect dominates the elbow dynamics. Therefore, as a standard procedure in the literature, offline least squares was employed to find the dynamic parameters M, B and K in the second-order model (1) according to

$$\mathbf{T}_h = \mathbf{P}[M, B, K]^T \quad \text{where} \tag{2}$$

$$\mathbf{P} = [\ddot{\boldsymbol{\theta}}_h,\ \dot{\boldsymbol{\theta}}_h,\ \Delta\boldsymbol{\theta}_h] \tag{3}$$

$$[\hat{M}, \hat{B}, \hat{K}] = (\mathbf{P}^T\ \mathbf{P})^{-1}\mathbf{P}^T\mathbf{T}_h \tag{4}$$

where the vectors $\Delta\boldsymbol{\theta}_h$, $\dot{\boldsymbol{\theta}}_h$, $\ddot{\boldsymbol{\theta}}_h$ and $\mathbf{T}_h$ represent the data collected over the entire length of the experiment. The hand and arm inertia were found after subtracting the pre-identified wrist clamp inertia from the identified total inertia. The computed inertia for all subjects, as displayed in Table I, are within the range of 0.0277 to 0.113 kgm^2 reported in the literature [4], [6].

B. Stiffness and Damping Identification

After finding the arm moment of inertia, the next step is to identify damping $B(\boldsymbol{\lambda}(t))$ and stiffness $K(\boldsymbol{\lambda}(t))$ in (1). Towards this goal, (1) is parameterized as

$$\mathbf{H}(t) = \mathbf{Y}(t)\mathbf{L}(t) \quad \text{where} \tag{5}$$

$$\mathbf{H}(t) = \mathbf{T}_h(t) - \mathbf{T}_h^*(t) - I\ddot{\boldsymbol{\theta}}_h(t) \tag{6}$$

$$\mathbf{Y}(t) = [\dot{\boldsymbol{\theta}}_h(t)\ \ \Delta\boldsymbol{\theta}_h(t)] \tag{7}$$

$$\mathbf{L}(t) = [B(\boldsymbol{\lambda}(t))\ \ K(\boldsymbol{\lambda}(t))]^T \tag{8}$$

where the vectors $\Delta\boldsymbol{\theta}_h(t)$, $\dot{\boldsymbol{\theta}}_h(t)$, $\ddot{\boldsymbol{\theta}}_h(t)$,$\mathbf{T}_h(t)$, $\mathbf{T}_h^*(t)$ and $\mathbf{H}(t)$ represent the data collected over an interval of time.

Since the frequency of random perturbations applied to elbow and the response of the arm dynamics are higher than the frequency of the voluntary background force generated directly by brain commands, to calculate $\mathbf{T}_h^*(t)$, the measured elbow torque $\mathbf{T}_h(t)$ is passed through a 100-tap FIR low-pass filter with cutoff frequency 5*Hz*. To compensate for the filtering delay, the resulting signal is shifted back in time by 50 samples. Afterwards, the calculated $\mathbf{T}_h^*(t)$ and the inertia term $M\dot{\boldsymbol{\theta}}_h(t)$ are subtracted from $\mathbf{T}_h(t)$ to calculate $\mathbf{H}(t)$ in (6). Since the inertial effect of wrist clamp was measured by force sensor, the total identified inertia for wrist clamp and forearm was used as $M(t)$.

To identify stiffness $K(\boldsymbol{\lambda}(t))$ and damping $B(\boldsymbol{\lambda}(t))$ at time t, a MWLS identification method is employed. In this

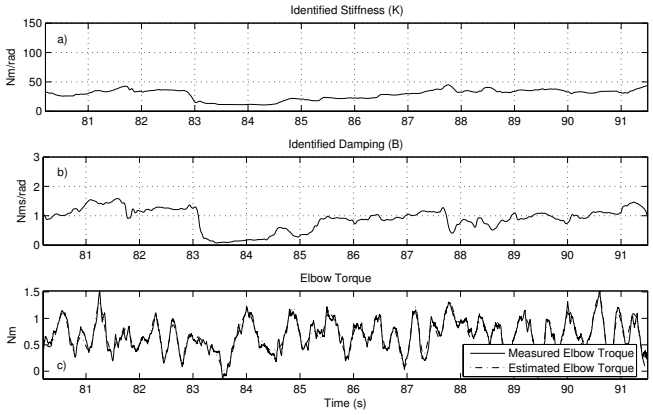

Fig. 4. Subject M1 identification results under experiment type II condition. a,b) Stiffness $K(t)$ and damping $B(t)$ using MWLS , c) elbow torque prediction using the identified quasi-linear model.

method, a moving window of $w+1$ torque and kinematic samples centered at time t are used for offline least square estimation $\mathbf{L}(t) = \mathbf{Y}(t)^T\mathbf{Y}(t))^{-1}\mathbf{Y}(t)^T\mathbf{H}(t)$. In our case, $w = 300$. After estimation the first and the last 300 samples are cut out to exclude the undesirable filtering effects. Figures 4.a,b display the identified stiffness and damping for subject M1 under experimental condition type II. These values are close to the range of damping [0.82-5.5] Nms/rad and stiffness [3-110] Nm/rad reported in the literature [1], [3], [4], [11]. The estimated torque $\hat{T}_h(t)$ using quasi-linear model (1) and the identified parameters are also compared to the torque applied to elbow Figure in 4.c. The average value of the Relative Mean Square Error (RMSE) defined as

$$RMSE \quad = \quad 100 * \frac{\Sigma_t (T_h(t) - \hat{T}_h(t))^2}{\sqrt{\Sigma_t T_h^2}\sqrt{\Sigma_t \hat{T}_h^2}} \qquad (9)$$

for all subjects and experimental condition types II and III are displayed in Table II.

Since the algorithm is trying to fit the best linear model parameters to the nonlinear dynamics of human arm, at few samples of the identified values become negative. Moreover, after statistical analysis of the collected data, it was observed that due to the stochastic nature of EMG signals, multiple stiffness or damping values were produced within a close vicinity of some operating points $\boldsymbol{\lambda}(t)$. Therefore, before training the RBFANN, the collected samples were preprocessed and reduced in number substantially according to a novel efficient algorithm to speed up the neighborhood search operation and search for redundant samples. Since the size of the 6D data matrix was very large (hundreds of megabytes), the data was reformatted into a 6×10^5 sparse matrix. The algorithm steps are briefly explained below:

1. The identification results with negative values, if any, were discarded.
2. The input values (4 EMG signals, angular position and velocity) were uniformly quantized to 20 points each within their dynamic range. Afterwards, the identification results for similar quantized input values were averaged after exclusion of any outlier. Input samples which were distant three times their standard deviation away from the sample mean were considered as outliers.
3. Impedance spatial outliers in the 6D variable space, spanned by quantized operating point vector, were discarded. Each identified value was determined as a spatial outlier if its difference with mean value of its neighboring samples was greater or smaller than 3 times of its standard deviation. The neighbor samples were samples whose Euclidian distance from the chosen sample in 6D space were smaller or equal to r (in this analysis $r = 3$).

TABLE II

TORQUE ESTIMATION ERROR USING QUASI-LINEAR MODEL.

Average RMSE	M1	M2	M3	M4
Type II	7%	10%	7%	11%
Type III	6%	3%	3%	3%

The above algorithm reduced the number of samples by 300 folds to approximately 2000 samples. Compared to the original sampled data and also evenly down sampled data, the use of quantized and refined data for training has improved the generalization performance of the RBFANN, which will be explained in the next section.

C. RBFANN-Based Impedance Estimator

The quantized 6D space spanned by the operating point vector $\boldsymbol{\lambda}(t) = [bi(t), tri(t), bra(t), radi(t), \theta_h(t), \dot{\theta}_h(t)]$ has a size of $20^6 = 6.4 \times 10^7$, where the arguments in the bracket refer to biceps EMG, triceps EMG, Brachialis EMG, Brachioradialis EMG, joint angle and angular velocity. However, since only the dynamic parameters of about 2000 cells are found using the MWLS identification method as described previously, the remaining cell values should be determined by interpolation/extrapolation among the available cells data. This is done using an RBFANN, which is known as a universal approximator and interpolator for nonlinear input-output mappings [8]. In this application, the inputs of RBFANN are EMG signals from biceps brachii, triceps, brachialis, and brachioradialis muscles, and elbow joint angle and velocity. The network output is the estimated impedance parameters, *i.e.* stiffness K or damping B, as illustrated Figure 1. In addition to the interpolation, RBFANN smooths the impedance function in the 6D quantized input space.

In the off-line training phase, the RBF network is presented with the network inputs and the identified impedance $\mathbf{L}(t)$ collected under experimental condition types II and III, which were refined by the search algorithm explained previously in this section. Two separate networks were trained for damping B and stiffness K. To find the optimal number of nodes for network hidden layer, networks were trained and validated against a second data set using impedance RMSE and Cross-Correlation (CC) criteria defined as

$$CC = 100 * \frac{\Sigma_i y_i * \hat{y}_i}{\sqrt{\Sigma_i y_i^2}\sqrt{\Sigma_i \hat{y}_i^2}}$$

TABLE III

RBFANN VALIDATION RESULTS FOR DAMPING B AND STIFFNESS K.

Averaged RMSE	M1	M2	M3	M4
Damping B				
RMSE	29%	53%	38%	35%
CC	83%	70%	78%	75%
Stiffness K				
RMSE	17%	34%	26%	29%
CC	91%	70%	87%	83%

where y_i and $\hat{y}_i$ are the measured and the estimated impedance parameters, respectively. Cross-correlation is a measure of similarity of the y and $\hat{y}$ profiles regardless of scaling. The closer the value is to 100, the higher the level of similarity is between the signals. It was found that 55 nodes for the estimation of B and 65 nodes for the estimation of K provided relatively maximum CC and minimum RMSE for validation results. Network training was terminated if the target mean square error 0.01% was met or the gradient became smaller than 10^{-10}.

The network validation results for B and K are displayed in Table III. The RBFANN estimate of B and K for subject M1 are displayed in Figures 5a,b. As it is expected, the output of the network is discrete. The reason is that the temporal neighboring input data are converted into similar values in the quantization process. Although the accuracy of parameter for K and especially B is not in the order of single digits, the online identified parameters clearly follow the pattern of changes in arm impedance. This level of accuracy can be enough for arm dynamic analysis and improved tradeoff between stability and performance in telerobotic and haptic control systems. One major factor in parameter error is the stochastic nature of EMG signals. The online estimation accuracy may be improved by changing the neural network input quantization level, and the use of more sensors for each muscle for more accurate representation of MALs.

It is expected that the network generated for each subject not be applicable to other subjects (inter-subject) and a separate network should be trained for each individual.

VI. CONCLUSION

In this work, a novel methodology for online estimation of human arm impedance for elbow motion in horizontal plane was proposed. The impedance was approximated with a second-order quasi-linear dynamic model using upper-arm EMG signals, and elbow angular position and velocity. The identification was conducted in three phases: i) the inertia of forearm and wrist were identified while subject was asked to relax all upper-arm muscles, ii) moving average least squares was employed to identify the stiffness and damping for a limited number of points, iii) an RBF artificial neural network was trained and used to approximate the impedance model parameters in the entire elbow operating space by interpolating/extraploating among the limited identified points found in (ii). In future, the possibility of achieving more accurate impedance estimates through the use of different neural network input quantization levels and the use of more EMG sensors on each muscle will be investigated. In addition, the identified impedance will be incorporated and tested in adaptive telerobotic and haptic control systems.

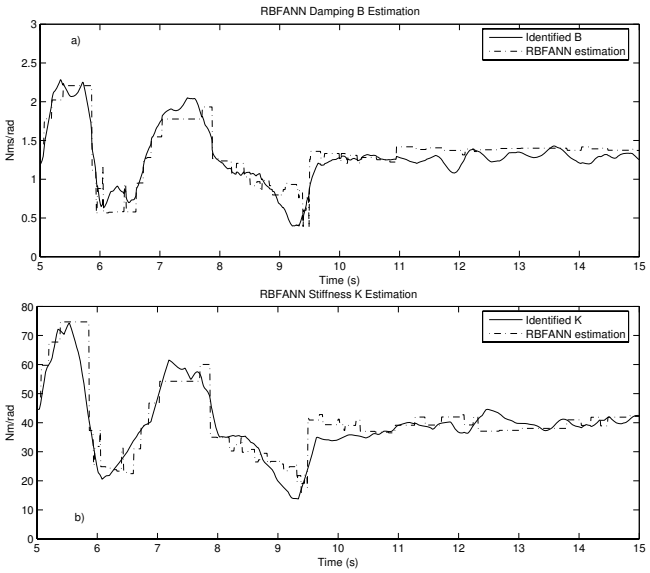

Fig. 5. RBFANN estimation results for Subject M1

ACKNOWLEDGMENT

This work was supported by Natural Sciences and Engineering Research Council of Canada (NSERC) and Institute for Robotics and Intelligent Systems (IRIS). The authors wish to thank Dr. Stephen Scott his collaboration and support in the design and construction of QArm1.

REFERENCES

[1] S. Stroeve, "Impedance characteristics of a neuromusculoskeletal model of the human arm i. posture control," *Biological Cybernetics*, no. 81, pp. 475–494, 1999.

[2] ——, "Impedance characteristics of a neuromusculoskeletal model of the human arm ii. movement control," *Biological Cybernetics*, no. 81, pp. 495–504, 1999.

[3] T. Tsuji and M. Kaneko, "Estimation and modeling of human hand impedance during isometric muscle contraction," in *Proceedings of the ASME Dynamic Systems and Control Division*, vol. 5, Atlanta, GA, November 1996, pp. 575–582.

[4] L. Zhang and W. Rymer, "Simultaneous and nonlinear identification of mechanical and reflex properties of human elbow joint muscles," *IEEE Trans on Biomed Eng*, vol. 44, pp. 1192–1209, 1997.

[5] R. Kearney and I. Hunter, "System identification of human joint dynamics," *Biomedical Engineering*, no. 18, pp. 55–87, 1990.

[6] Y. Xu and J. Hollerbach, "Identification of human joint mechanical properties from single trial data," *IEEE Transactions on Biomedical Engineering*, vol. 45, no. 8, pp. 1051 – 1060, August 1998.

[7] D. Franklin, F. Leung, M. Kawato, and T. Milner, "Estimation of multijoint limb stiffness from emg during reaching movements," in *Proceedings of IEEE EMBS Asian-Pacific Conference on Biomedical Engineering*, 2003, pp. 224 – 225.

[8] F. Girosi, M. Jones, and T. Poggio, "Regularization theory and neural networks architectures," *Neural Computation*, pp. 219–269, 1995.

[9] F. Mobasser and K. Hashtrudi-Zaad, "Hand force estimation using electromyography signals," in *Proceedings of IEEE International Conference on Robotics and Automation*, 2005, pp. 2642–2647.

[10] C. D. Luca, "The use of surface electromyography in biomechanics," *Journal of Applied Biomechanics*, vol. 13, pp. 135–163, 1997.

[11] T. Flash and F. Mussa-Ivaldi, "Human arm stiffness characteristics during the maintenance of posture," *Experimental Brain Results*, no. 82, pp. 315–327, 1990.